Applied Surface Science 379 (2016) 264–269

Contents lists available at ScienceDirect

Applied Surface Science

journal homepage: www.elsevier.com/locate/apsusc

Surface modification of multiwall carbon nanotubes by sulfonitric treatment

Sofía Gómez[a,*], Nicolás M. Rendtorff[a,b], Esteban F. Aglietti[a,b], Yoshio Sakka[c], Gustavo Suárez[a,b]

[a] Centro de Tecnología de Recursos Minerales y Cerámica (CETMIC), Camino Centenario y 506, C.C.49, M.B. Gonnet B1897ZCA, Argentina
[b] Departamento de Química, Facultad de Ciencias Exactas—UNLP, Calle 115 y 47, La Plata 1900, Argentina
[c] National Institute for Materials Science, Tsukuba, Ibaraki 305-0047, Japan

ARTICLE INFO

Article history:
Received 7 January 2016
Received in revised form 28 March 2016
Accepted 10 April 2016
Available online 12 April 2016

Keywords:
Carbon nanotubes
Acid treatment
Surface modification

ABSTRACT

Carbon nanotubes are widely used for electronic, mechanical, and optical devices due to their unique structural and quantum characteristics. The species generated by oxidation on the surface of these materials permit binding new reaction chains, which improves the dispersibility, processing and compatibility with other materials.

Even though different acid treatments and applications of these CNT have been reported, relatively few research studies have focused on the relationship between the acid treatment and the formation of nanodefects, specific oxidized species or CNT surface defects.

In this work, multiwall carbon nanotube (MWCNT) oxidation at 90 °C was characterized in order to determine the acid treatment effect on the surface.

It was found that oxidized species are already present in MWCNT without an acid treatment, but there are not enough to cause water-based dispersion. The species were identified and quantified by infrared spectroscopy and X-ray photoelectron spectroscopy. Also, transmission electron microscopy observations showed not only modifications of the oxidized species, but also morphological damage on the surfaces of MWCNT after being subjected to the acid treatment. This effect was also confirmed by Raman spectroscopy. The acid treatment generates higher oxidized species, decreasing the zeta potential in the whole pH range.

1. Introduction

Carbon nanotubes (CNT) are widely used for electronic, mechanical, and optical devices due to their unique structural and quantum characteristics [1–3]. But in order to explore their potential applications, functionalization of the nanotubes is necessary.

In ceramic science, multiwall carbon nanotubes (MWCNT) can be used as reinforcement in nanostructured ceramic matrices to make them stronger and lighter [4]. The main drawback is the homogeneous dispersion of the MWCNT in the ceramic matrix. Several factors play an important role in the dispersion and distribution. The surface characteristics of these MWCNT make them difficult to disperse in water-based suspension and, in consequence, difficult to generate homogeneous ceramic composites containing MWCNT.

These materials are hydrophobic and chemically inert, particularly when pristine MWCNT maintain the rolled graphene structure. Many technological applications aim at tailoring their properties by functionalizing the surface.

Covalent addition of carboxylic groups to the surface of the MWCNT is one common way to achieve further covalent functionalization of nanotubes. The major difficulty is that oxidative functionalization results in the formation of several different chemical functions containing oxygen groups such as carboxylic, carbonyl, ether, ketone and other groups that can form on the MWCNT surface [5–8].

The dispersion of carbon nanotubes is influenced by the nature of the surface, as they usually agglomerate due to interactions between themselves. Surface modification of MWCNT using acids seeks to achieve their good dispersion and distribution in the final material, improving their properties and potential uses.

* Corresponding author.
E-mail addresses: sofiagomez@cetmic.unlp.edu.ar (S. Gómez), rendtorff@cetmic.unlp.edu.ar (N.M. Rendtorff), eaglietti@cetmic.unlp.edu.ar (E.F. Aglietti), SAKKA.Yoshio@nims.go.jp (Y. Sakka), gsuarez@cetmic.unlp.edu.ar (G. Suárez).

http://dx.doi.org/10.1016/j.apsusc.2016.04.065
0169-4332/

The species generated by oxidation on the surface of these materials permit binding new reaction chains, which improves the solubility, processing and compatibility with other materials. The homogeneous dispersion of MWCNT allows their use in composites using different ceramic matrices and as composite components.

When attacked by a sulfonitric mixture, MWCNT undergo some oxidative cleavage of carbon-carbon bonds converting sp2 hybridized carbon atoms into oxidized sp3 ones on the surface and forming oxidized species that provide a highly negative zeta potential even at acid pH [9]. Consequently, good dispersion in the slurry is obtained [4,10,11].

Yamamoto et al. have successfully introduced nanoscale defects on the MWCNTs surface using acid treatment on the pristine nanotubes to disperse the MWCNTs homogeneously in the matrix and improve the connectivity between MWCNTs and the matrix. The rationale behind the acid treatment is to introduce nanoscale defects and adsorb negatively charged functional groups at the MWCNT ends and along their lengths. They demonstrated that the pristine MWCNTs have a high crystalline multi-walled structure with no defects on the wall surface and no significant overall damage took place in the MWCNTs during the acid treatment. A homogeneous distribution of nanotubes in an alumina matrix has been achieved by acid-treated MWCNTs. Combined with a mechanical interlock induced by the chemically modified CNTs, this approach leads to improved mechanical properties [12].

Even though different acid treatments and applications of these MWCNT have been reported, relatively few research studies have focused on the relationship between the acid treatment and the formation of nanodefects, specific oxidized species or MWCNT surface defects.

Zhou et al. reported [9] nanodefects produced by a sulfonitric mixture at 373 K, as revealed by TEM observations, Raman spectroscopy and FTIR measurements. Nishikori et al. [13] performed oxidation studies using an acidic mixture and employed XPS and the UV–vis absorption method using 1-aminopyrene as a fluorescent probe.

In spite of the different acid treatments and analytical techniques employed, there are still many conflicts in the literature concerning the analysis and study of the oxide species formed on the MWCNT surface.

The effect of the acid treatment is more than clear and justified because of the many applications that allow obtaining a modified surface capable of reacting, dispersing and being used as required, but the difficulty of characterization techniques as well as different reaction conditions make it difficult to understand and control the final species formed on the MWCNT surface.

In this work, in order to clarify and compare different analytical techniques, MWCNT oxidation at 90 °C was studied in order to determine the acid treatment effect on the surface. XPS (X-ray photoelectron spectroscopy), FTIR (Fourier transform infrared spectroscopy), XRD (X-ray diffraction), Raman spectroscopy, TEM (transmission electron microscopy) and zeta potential were used.

2. Material and methods

Commercial multiwall carbon nanotubes (Bussan Nanotech, Ibaraki, Japan; diameter 20–70 nm) were used. A H_2SO_4 98% and HNO_3 65% (3:1 v/v) solution was employed for the acid treatment of 1.25 g of MWCNT under vigorous stirring for 20 min at 90 °C. The oxidative species are produced as shown in Fig. 1.

Finally, the acid mixture is diluted, cooled down and washed out up to near neutral pH. The washed suspension is dried at 60 °C for three days and finally, at 110 °C up to constant weight.

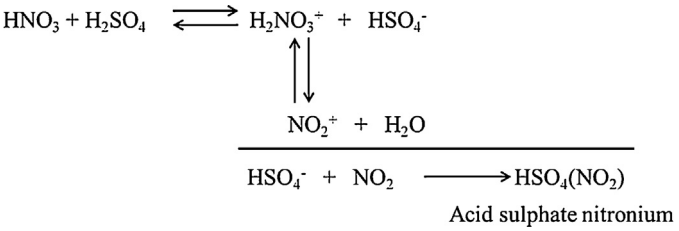

Fig. 1. Oxidation agent produced by the sulfonitric mixture.

In order to analyze the effect of the acid treatment on the MWCNTs and compare them with the original (pristine) MWCNT, different analytical techniques were used.

X-ray photoelectron spectroscopy was used with an XR50, SPECS and a hemispheric energy analyzer PHOIBOS 100 MCD with Mg Kα (1253.6 eV) radiation, operating at 13 KV 300 W in an energy fixed analyzer transmission (FAT) mode. FTIR was also used to analyze the surface modification with an IR-BrukerVertex 70 in the wavelength range 500–4000 cm^{-1}. The crystallographic analysis was performed with X-ray diffraction equipment Philips 3020. The XRD pattern was recorded in the range between 10 and 70° (2θ), step of 0.04° and 2 s per step. Raman spectroscopy was recorded with a Raman Jobin Yvon Lab HR-Raman at a wavelength of λ = 514.53 nm. The intensities were estimated as Lorentzian functions.

The changes in zeta potentials were measured in deionized water varying pH between using a zeta potential analyzer (Zeta Plus, Zeta Potential, Brookhaven Instruments Corporation, USA). The pH value of the aqueous solution was adjusted with HCl and NaOH in the 3–11 pH range.

The pristine and treated MWCNTs were morphologically and texturally characterized by transmission electron microscope Zeiss EM109 Turbo.

3. Results

3.1. XRD analysis

Fig. 2 shows the typical XRD pattern of the MWCNT. The strongest diffraction peak at the angle (2θ) of 25.5° can be indexed as the (002) reflection of the hexagonal highly ordered graphite structure [14–17]. The decrease in sharpness of the peak at 25.5° (2θ) indicates that the graphite structure of the treated MWCNT was acid-oxidized without significant damage since any decrease in the crystallinity order of MWCNT will make the XRD peaks broader

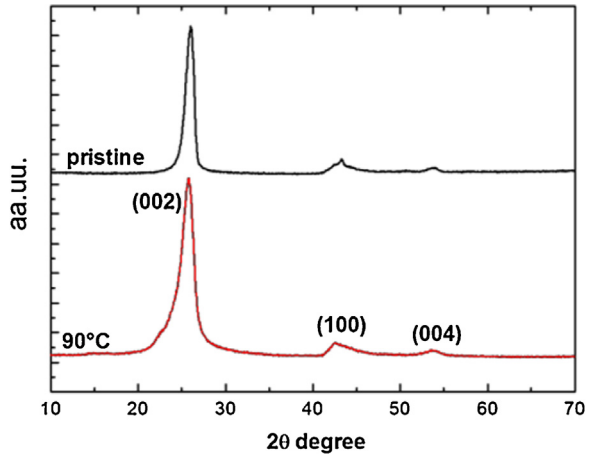

Fig. 2. XRD pattern of pristine and treated at 90 °C MWCNT.

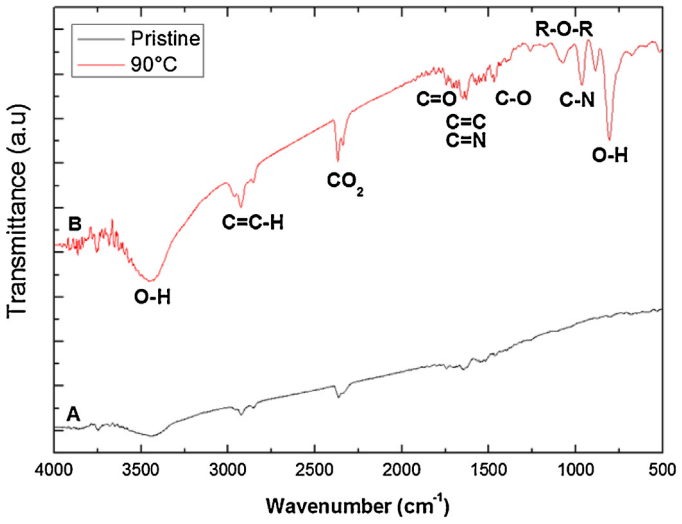

Fig. 3. FTIR of pristine and treated at 90 °C MWCNT.

and shifts the peak diffraction towards lower angles. The other characteristic diffraction peaks of graphite at 2θ of about 43° and 53° are associated with C (100) and C(004) diffractions of graphite, respectively. However, the absence of any sign of (101) can be considered to be due to the lack of three-dimensional stacking as in graphene.

The acid treatment under the above-described conditions generates oxidation on the surface, which is not clearly evident by XRD observations due to the non-crystalline nature of these modifications. However, some differences can be observed. XRD analyzes the atomic order of the overlapped rolled graphene layers that form the nanotubes, and it can be seen in Fig. 2 that some peaks are broadened due to the surface disorder produced by the acid attack. This effect appears on the surface and does not affect the crystallinity; the position and intensity of the peaks is the same. No new crystalline species, salts or any other diffraction signals are present.

3.2. FTIR surface characterization

FTIR is a qualitative technique that allows identifying functional groups in the exterior layer of the MWCNT. The spectra of pristine and oxidized at 90 °C MWCNT are compared in Fig. 3. The peaks in the pristine MWCNT show evidence of oxidized species, but are considerable weaker than in the treated one. This effect might be due both to effective oxidation on the surface and the fact that FTIR is more effective on oxidized species [18,19].

The band at 2949 cm^{-1} corresponds to the symmetric stretching of C—H bonds in carbonaceous material (*ν*s. C—H). The spectra show intensive bands near 3500 cm^{-1} (stretching vibrations of isolated surface —OH substituents and/or —OH of carboxyl groups and of sorbed water). The shifts in characteristic wavenumbers to lower wavenumbers indicate the presence of strong hydrogen bonds between —OH groups. The bands in the 1750–1550 cm^{-1} range can be assigned to C=O groups in different environments (carboxylic acid, ketone/quinone) and to C=C in aromatic rings, whereas the bands in the range 1300–950 cm^{-1} confirm the presence of C—O bonds coming from various chemical surroundings. The 2300 cm^{-1} band can be attributed to CO_2 adsorbed on the sample.

Also, a band at 1550 cm^{-1} can be seen, most probably due to aromatic and unsaturated structural C=C bonds. The band near 1410 cm^{-1} can be assigned to the C—O bond present in C—O—C groups containing oxygen bridges.

Table 1
Assignments of the C1s spectra fitting into C and O chemical groups for XPS spectra of pristine and after acid treatment at 90 °C CNT (the results are expressed in%).

Peak	1	2	3	4	5
B.E./eV	284.4	285.5	286.8	288.9	291.3
Bonds assignments	C-C C-H	C-OH C-N C-O-C	C=O N-C-O C-C \ / O	C=O \ O-R	π-π* (shake up)
pristine	63.0%	23.7%	4.6%	4.6%	4.1%
treat at 90°C	64.0%	16.1%	5.8%	9.9%	4.3%

As a result of oxidation, the intensity of the —OH band assigned to the associated water (3444 cm^{-1}) and the appearance of oxidized species peaks confirm the presence of various oxidations in the original pristine MWCNT. The C=O bands characteristic of carboxylic functional groups (—COOH) and of ketone/quinone are observed at 1711 and 1638 cm^{-1}, respectively [20]. The relative increase in the bands in the 1250–950 cm^{-1} wave region indicates an increase in the amounts of hydrated surface oxides.

The presence of C—N bonds could be identified by the band at 1244 cm^{-1}, which possibly derived from the stretching of C—N bonds (*ν*C—N). The incorporation of N-atoms into the graphitic lattice could be confirmed by a signal at 1580 cm^{-1} from a mixed stretching mode of C=N and C=C (*ν*C=N + C=N), which was shifted to lower wavenumbers as compared to the signal from aromatic C=C bonds. These findings are in agreement with previous reports [21–24], which demonstrated that the replacement of carbon atoms with nitrogen atoms in the sp2 networks induces a strong IR activity. Consequently, absorption in the 1200–1600 cm^{-1} regions would be expected if N-atoms were covalently bonded to the carbon network.

The 1050 and 1300 cm^{-1} peaks correspond to the C—O (and —OH) vibrations from alcohols, ether and presumably oxidative anhydride or carboxylic [25] products of the external graphite layers.

3.3. XPS

The XPS spectra are obtained by irradiating a material with a beam of X-rays while simultaneously measuring the kinetic energy and number of electrons that escape from the top 0–10 nm of the material being analyzed. The survey XPS C1s spectra recorded from the commercial MWCNT sample with and without acid treatment show mainly carbon and oxygen species contents (Fig. 4). The surface atomic content from the analysis of the C1s spectra area after background subtraction [26], assuming homogeneous distribution of atoms, was analyzed.

The curves for each oxidized group formed in the MWCNT can be observed. The analysis and quantification of XPS results are shown in Table 1, which lists the possible band assignments of the two samples and the atomic percentages of the oxidized species in the two samples studied.

The oxidized species in the pristine MWCNT may have formed during the manufacturing process [18]. There are a larger number of carboxylic and carbonyl groups in the treated MWCNTs than in the pristine ones.

Table 1 also shows the quantitative analysis of the oxidized species and the sequential oxidation process.

The C1s core line is fitted, and these binding energy peaks are assigned to sp^2 C=C (284.3–284.4 eV), sp3 C—C (285.1–285.3 eV), C—O at 286.8 eV, C=O at 287.1 eV, ester groups (O—C=O) at 288.9 eV and π-π* at 291.3 eV [27,28].

The pristine MWCNT has the highest percentage of detected species in the XPS spectra including C—C and/or C—H and C—OH,

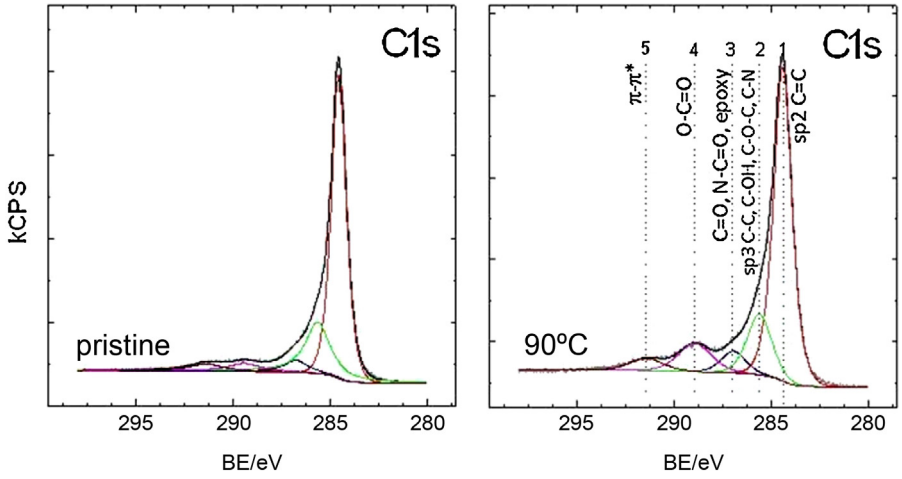

Fig. 4. C1s spectra fitting into C and O chemical groups for the XPS spectra recorded for treated at 90 °C and pristine MWCNT.

C—O—C and C—N assignments. As it was mentioned above, they are oxidized species produced during the manufacturing process. The treated CNT presents a lower amount of C—OH, C—O—C and C—N, but a higher quantity of C═O, N— C═O, COOR, which indicates that those species are formed from the basic oxidized species as part of a sequential oxidation process that starts first in the C—C and C—H bonds and then continues to the other species listed in Table 1. The values for C═O and C—O groups, with an overlap between double C═O (carbonyl, carboxyl) and single C—O (hydroxyl, carboxyl, epoxy) bonds depend on the synthesis of the MWCNT and the thermochemical treatment during the acid treatment of them.

The first column of Table 1 lists the assignments for the C—C and C—H bonds, which are the highest due to the fact that MWCNTs consist of rolled concentric graphite layers.

These bonds generate the aforementioned oxidative groups and others such as carbonyl, aldehyde, ether, ester and carboxylic acids groups.

Stobinski et al. [29] used a 120 °C acid treatment with HNO_3 and by XPS analysis and FTIR observed oxidized species on the surface. Daoush and Hong [30] reported a different acid treatment (mix of acids at 50 °C) and found the same oxidized species listed in Table 1.

It is clear that the acid treatment generates oxidation. The results are difficult to compare quantitatively because of the different process conditions, temperature, acid concentration and treatment time, but the oxidized species responsible for the dispersion in water-based suspension were identified by XPS.

This analysis shows the same species observed previously by FTIR, supporting the observation of MWCNT surface oxidation after the acid treatment.

The π–π^* transition of the MWCNT is slightly affected by the acid treatment, as is shown in Table 1.

3.4. Raman spectroscopy

Raman spectroscopy is a tool to characterize carbonaceous materials and evaluate disorders in their structures [31].

Fig. 5 shows the Raman spectra of the pristine and treated MWCNT. In both cases the characteristics peak at 1360 cm^{-1}, corresponding to the D band, and the other one at 1590 cm^{-1}, corresponding to the G band in the Raman shift between 1200 and 1800 cm^{-1}, can be observed. It is well known that the D-band is caused by a double resonance scattering due to the presence of structural defects, while the G-band originates from tangential in-plane vibration of graphitic carbon atoms [32]. Also, the G-band in the Raman spectrum of MWCNTs sometimes appears with a high frequency shoulder that is known as Dí-band [33]. Like the D-band,

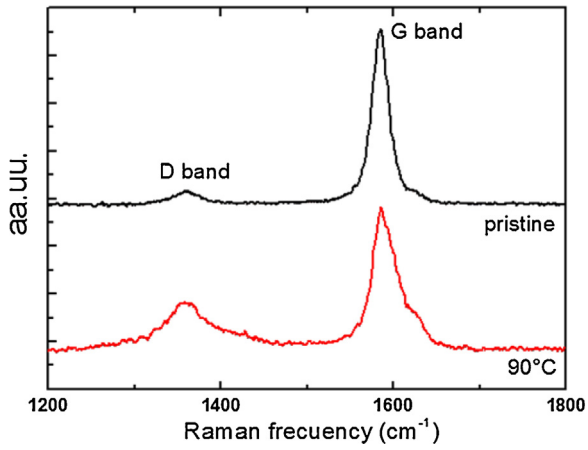

Fig. 5. Raman spectroscopy of the pristine and treated MWCNT.

Table 2
Position of the G and D bands, as well as the ratio between intensities ID/IG for both pristine and treated MWCNT.

	Raman frequency (cm^{-1})	I_D/I_G	
pristine	G	1360	0.1
	D	1585	
treat at 90 °C	G	1362	0.7
	D	1590	

the Dí-band is also a double-resonance band induced by disorder and defects.

In conclusion, the D-band is associated with the disorder of graphite and the G-band with the order in the crystalline structure.

Table 2 shows the position of the G and D bands, as well as the ratio between intensities, ID/IG. This ratio depends on the structural relation of the carbon material [34]. ID/IG can be used as a parameter to approximate the order degree of the number of defects present on the CNT surface [35]. A high value of this ratio means defects on the carbon surface and low degree of graphitization [36]. It was found that the ID/IG ratio increases considerably after the acid treatment, as can be seen in Table 2. This can be translated into damage by acid attack and can be observed also by TEM in Section 3.6.

Motchelaho et al. [19] performed an acid treatment at 120 °C varying the time and the HNO_3 proportion and correlating the effect of the treatment on the surface damage with TEM and Raman spec-

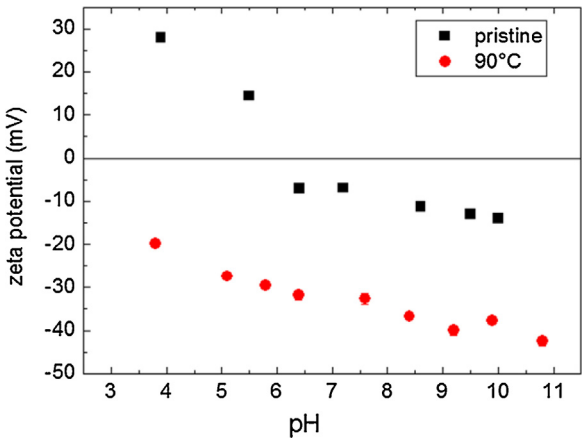

Fig. 6. Zeta potential of treated (90 °C) and pristine MWCNT as a function of pH.

troscopy. The ID/IG ratio is also higher for the treated MWCNT. Fraczek- Szcypta [37] used H_2SO_4 and HNO_3 with a volumetric ratio (3:1, respectively) at 60 °C and 70 °C. The ID/IG ratio is also high after the acid treatment and is explained as a decrease in crystallinity.

3.5. Zeta potential

The zeta potential of the MWCNT water suspension can also be studied to correlate the oxidized species on the surface and their effect on the actual behavior in suspension. Fig. 6 shows the variation of the zeta potential as a function of pH.

The presence of carboxylic groups on the MWCNT surface turns the nanotubes hydrophilic, causing an increase in the negative charge and also shifting the isoelectric point to lower pH values, as shown in the zeta potential measurement.

For the pristine MWCNT, the isoelectric point is near pH 6, which means that at a lower pH, the surface is charged positively. The surface of the nanotubes in acidic media (pH 3–6) is positively charged due to the presence of the oxidized species (OH— and COOH— groups) present in the original MWCNT.

After the acid treatment at 90 °C, the isoelectric point is not reached at the pH range evaluated. The surface charge is negative and the isoelectric point is not reached in that range due to the oxidized negative species on the MWCNT surface. An increase in the number of oxidized specimen and a decrease in the number of low oxidized groups formed on the surface (as a result of oxidation) do not overcompensate for the positive surface charge. At least not at low pH values where the weak acidic groups either acquire positive charge due to proton transfer from the solution or their dissociation gets suppressed.

The surface of the MWCNT sample oxidized by H_2SO_4/HNO_3 mixture is negatively charged in a wide range of pH values (3–11), which can be explained by two factors: first, the increasing dissociation of the surface groups results in a constant increase; second, the suppression of the diffuse double layer is accompanied by a decrease in the absolute zeta potential [38].

In the processing of composite materials the negative surface of MWCNT makes the attached thereof to the ceramic matrix is reinforced by an electrostatic effect. Furthermore Yamamoto et al. have used the acid treatment to introduce nanoscale defects on the surface of the MWCNT and they demonstrated that those defects have been effective in reinforcing structural ceramic components. They measure the tensile strength ranged from ~2 to ~48 GPa for the pristine MWCNTs and for the acid-treated MWCNTs, measured strengths ranged from ~1 to ~18 GPa. These results suggest that the more effective interlocking of the 'notched' MWCNTs (from acid treatment), in the composites, more than offsets the reduction in tensile strength of acid-treated vs. pristine MWCNTs of this type [39].

3.6. Morphological analysis by TEM

Fig. 7 shows TEM micrographs of pristine (A) and treated at 90 °C (B) MWCNT.

Fig. 7B shows clear surface modification and damage on the MWCNT exterior wall. Fig. 7B depicts the detrimental effect on the surface of the acid treated nanotubes. Also it can be observed that some of the MWCNT present a higher oxidation effect on the tip, which can be because the C=C bonds break, resulting in an open end. These changes indicate that the acid treatment generates not only chemical but also morphological changes.

Zhou et al. [9] studied the control of the nanodefects produced by acid treatment and they found that after 30 min of oxidation at 50 °C (323 K) groove type defects are formed on the outer wall of the CNTs, but their number is very limited.

The pristine MWCNT surface (Fig. 7A) shows no destruction on the walls. The acid treatment (Fig. 7B) created defects that resulted in damaged on the walls, but no shortening was observed.

Yudianti el al [40]. reported that the acid treatments at 100 °C generates nanodefects on the CNT walls, and they estimated a shortening of 200–500 nm in length. Liu et al. [8] also used a mixture of H_2SO_4/HNO_3 to cut the highly tangled long MWCNT into shorter, open-ended tubes and thus produced many carboxylic groups at the open end. Zhang et al. [41] stated that acidic treatment is known to intercalate and exfoliate graphene, creating a higher number of oxidation sites on carbon atoms. The oxidation site might be formed on the side wall and at the end of the tube as discussed by Chen et al. [42]. Finally, Marshall et al. [43] observed a cutting effect on single-wall CNT with an acid treatment and ultrasonication at room temperature. This cutting effect can be due to the fact that CNT are

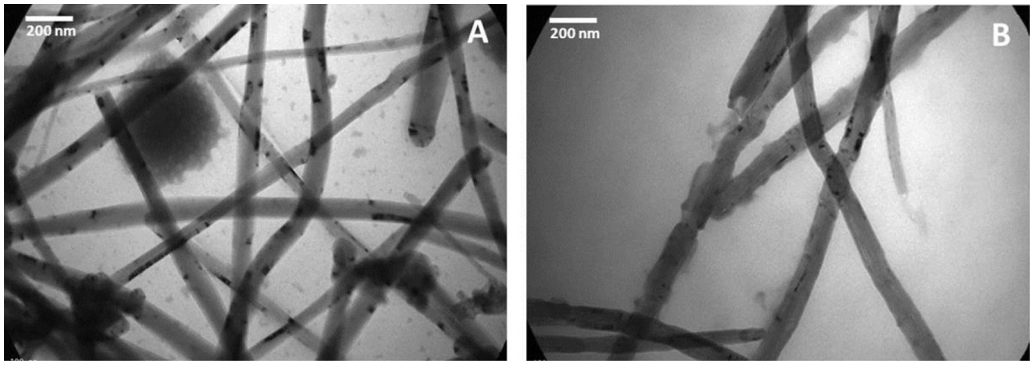

Fig. 7. TEM micrographs of pristine MWCNT (A) and MWCNT treated at 90 °C for 20 min (B).

single wall and moreover, the time used by that research group was not shorter than 2 h. In the present work, the acid treatment time was 20 min. In all the morphological surface analyses based on TEM images in this work, nanotubes present some surface defects but no shortening. This proves that the acid treatment can generate functional groups on the surface, but no shortening.

4. Conclusions

The sulfonitric treatment of multiwall carbon nanotubes (MWCNT) was studied using different techniques involving both surface and structural (FTIR, Raman spectroscopy, XPS, zeta potential and TEM observations) analyses. The different techniques used showed that the pristine MWCNT already presents oxidized species that are highly oxidized such as carbonylic or carboxylic groups after the oxidative process. The oxidation of these MWCNT brings along the modification of the zeta potential and also generates a high negative charge of the MWCNT in all the pH range.

After treatment, the MWCNT exterior walls show slight deterioration, as revealed by TEM observations and Raman spectroscopy. This effect is translated into a good dispersion of the nanotube in water-based suspension avoiding agglomeration and making the suspension suitable for composite preparation. Some surface defects but no shortening were observed by TEM images.

References

[1] M. Endo, Y.A. Kim, T. Hayashi, Y. Fukai, K. Oshida, M. Terrones, et al., Structural characterization of cup-stacked-type nanofibers with an entirely hollow core, Appl. Phys. Lett. 80 (7) (2002) 1267–1269.

[2] M. Endo, Y.A. Kim, T. Hayashi, K. Nishimura, T. Matusita, K. Miyashita, et al., Vapor-grown carbon fibers (VGCFs)—basic properties and their battery applications, Carbon 39 (9) (2001) 1287–1297.

[3] T.T. Tan, H.S. Sim, S.P. Lau, H.Y. Yang, M. Tanemura, J. Tanaka, X-ray generation using carbon-nanofiber-based flexible field emitters, Appl. Phys. Lett. 88 (10) (2006).

[4] A.L. Martínez-Hernández, C. Velasco-Santos, V.M. Castaño, Carbon nanotubes composites: processing, grafting and mechanical and thermal properties, Curr. Nanosci. 6 (1) (2010) 12–39.

[5] A. Barinov, O.B. Malcioğlu, S. Fabris, T. Sun, L. Gregoratti, M. Dalmiglio, et al., Initial stages of oxidation on graphitic surfaces: photoemission study and density functional theory calculations, J. Phys. Chem. C 113 (21) (2009) 9009–9013.

[6] M.A. Hamon, H. Hu, P. Bhowmik, S. Niyogi, B. Zhao, M.E. Itkis, et al., End-group and defect analysis of soluble single-walled carbon nanotubes, Chem. Phys. Lett. 347 (1–3) (2001) 8–12.

[7] M.A. Hamon, H. Hui, P. Bhowmik, H.M.E. Itkis, R.C. Haddon, Ester-functionalized soluble single-walled carbon nanotubes, Appl. Phys. A: Mater. Sci. Process. 74 (3) (2002) 333–338.

[8] J. Liu, A.G. Rinzler, H. Dai, J.H. Hafner, R. Kelley Bradley, P.J. Boul, et al., Fullerene pipes, Science 280 (5367) (1993) 1253–1256.

[9] W. Zhou, S. Sasaki, A. Kawasaki, Effective control of nanodefects in multiwalled carbon nanotubes by acid treatment, Carbon 78 (2014) 121–129.

[10] F. Ahmadpoor, S.M. Zebarjad, K. Janghorban, Decoration of multi-walled carbon nanotubes with silver nanoparticles and investigation on its colloid stability, Mater. Chem. Phys. 139 (1) (2013) 113–117.

[11] S.C. Tsang, Y.K. Chen, P.J.F. Harris, M.L.H. Green, A simple chemical method of opening and filling carbon nanotubes, Nature 372 (6502) (1994) 159–162.

[12] G. Yamamoto, M. Omori, T. Hashida, H. Kimura, A novel structure for carbon nanotube reinforced alumina composites with improved mechanical properties, Nanotechnology 19 (2008) 7, 315708.

[13] H. Nishikiori, T. Tanigaki, M. Endo, T. Fujii, Quantitative characterization of acidic groups on acid-treated multi-walled carbon nanotubes using 1-aminopyrene as a fluorescent probe, Carbon 66 (2014) 560–566.

[14] C. Lu, F. Su, S. Hu, Surface modification of carbon nanotubes for enhancing BTEX adsorption from aqueous solutions, Appl. Surf. Sci. 254 (21) (2008) 7035–7041.

[15] I.D. Rosca, F. Watari, M. Uo, T. Akasaka, Oxidation of multiwalled carbon nanotubes by nitric acid, Carbon 43 (15) (2005) 3124–3131.

[16] T. Saleh, M. Dahmardeh, A. Bsoul, A. Nojeh, K. Takahata, Field-emission-assisted approach to dry micro-electro-discharge machining of carbon-nanotube forests, J. Appl. Phys. 110 (10) (2011).

[17] T.A. Saleh, The influence of treatment temperature on the acidity of MWCNT oxidized by HNO_3 or a mixture of HNO_3/H_2SO_4, Appl. Surf. Sci. 257 (17) (2011) 7746–7751.

[18] B.C. Satishkumar, A. Govindaraj, J. Mofokeng, G.N. Subbanna, C.N.R. Rao, Novel experiments with carbon nanotubes: opening, filling, closing and functionalizing nanotubes, J. Phys. B: At. Mol. Opt. Phys. 29 (21) (1996) 4925–4934.

[19] M.A.M. Motchelaho, H. Xiong, M. Moyo, L.L. Jewell, N.J. Coville, Effect of acid treatment on the surface of multiwalled carbon nanotubes prepared from Fe-Co supported on $CaCO_3$: Correlation with Fischer-Tropsch catalyst activity, J. Mol. Catal. A: Chem. 335 (1–2) (2011) 189–198.

[20] S. Biniak, A., Swiatkowski, M. Walczyk, in: A.P. Terzyk, P.A. Gauden, Carbon Materials: Theory and Practice, in Carbon Materials, P. Kowalczyk, Ed. 2008: India. p.51.

[21] S. Boncel, S.W. Pattinson, V. Geiser, M.S.P. Shaffer, K.K.K. Koziol, En route to controlled catalytic CVD synthesis of densely packed and vertically aligned nitrogen-doped carbon nanotube arrays, Beilstein J. Nanotechnol. 5 (1) (2014) 219–233.

[22] J.H. Kaufman, S. Metin, D.D. Saperstein, Symmetry breaking in nitrogen-doped amorphous carbon: infrared observation of the Raman-active G and D bands, Phys. Rev. B 39 (18) (1989) 13053–13060.

[23] S.H. Lai, Y.L. Chen, L.H. Chan, Y.M. Pan, X.W. Liu, H.C. Shih, The crystalline properties of carbon nitride nanotubes synthesized by electron cyclotron resonance plasma, Thin Solid Films 444 (1–2) (2003) 38–43.

[24] M.R. Wixom, Chemical preparation and shock wave compression of carbon nitride precursors, J. Am. Ceram. Soc. 73 (7) (1990) 1973–1978.

[25] S. Kundu, Y. Wang, W. Xia, M. Muhler, Thermal stability and reducibility of oxygen-containing functional groups on multiwalled carbon nanotube surfaces: a quantitative high-resolution XPS and TPD/TPR study, J. Phys. Chem. C 112 (43) (2008) 16869–16878.

[26] L. Stobinski, B. Lesiak, A. Malolepszy, M. Mazurkiewicz, B. Mierzwa, J. Zemek, P. Jiricek, I. Bieloshapka, Graphene oxide and reduced graphene oxide studied by the XRD, TEM and electron spectroscopy methods, J. Electron Spectrosc. Relat. Phenom. 195 (2014) 145–154.

[27] Y.L. Huang, S.M. Yuen, C.C.M. Ma, C.Y. Chuang, K.C. Yu, C.C. Teng, et al., Morphological, electrical, electromagnetic interference (EMI) shielding, and tribological properties of functionalized multi-walled carbon nanotube/poly methyl methacrylate (PMMA) composites, Compos. Sci. Technol. 69 (11–12) (2009) 1991–1996.

[28] X. He, F. Zhang, R. Wang, W. Liu, Preparation of a carbon nanotube/carbon fiber multi-scale reinforcement by grafting multi-walled carbon nanotubes onto the fibers, Carbon 45 (13) (2007) 2559–2563.

[29] L. Stobinski, B. Lesiak, L. Kövér, J. Tóth, S. Biniak, G. Trykowski, et al., Multiwall carbon nanotubes purification and oxidation by nitric acid studied by the FTIR and electron spectroscopy methods, J. Alloys Compd. 501 (1) (2010) 77–84.

[30] W.M. Daoush, S.H. Hong, Synthesis of multi-walled carbon nanotube/silver nanocomposite powders by chemical reduction in aqueous solution, J. Exp. Nanosci. 8 (5) (2013) 578–587.

[31] M. Endo, K. Nishimura, Y.A. Kim, K. Hakamada, T. Matushita, M.S. Dresselhaus, et al., Raman spectroscopic characterization of submicron vapor-grown carbon fibers and carbon nanofibers obtained by pyrolyzing hydrocarbons, J. Mater. Res. 14 (12) (1999) 4474–4477.

[32] M.S. Dresselhaus, G. Dresselhaus, R. Saito, A. Jorio, Raman spectroscopy of carbon nanotubes, Phys. Rep. 409 (2) (2005) 47–99.

[33] K. Behler, S. Osswald, H. Ye, S. Dimovski, Y. Gogotsi, Effect of thermal treatment on the structure of multi-walled carbon nanotubes, J. Nanopart. Res. 8 (5) (2006) 615–625.

[34] J. Kastner, T. Pichler, H. Kuzmany, S. Curran, W. Blau, D.N. Weldon, et al., Resonance Raman and infrared spectroscopy of carbon nanotubes, Chem. Phys. Lett. 221 (1–2) (1994) 53–58.

[35] G. Katagiri, H. Ishida, A. Ishitani, Raman spectra of graphite edge planes, Carbon 26 (4) (1988) 565–571.

[36] J. Lu, G. Wang, L. Sun, F. Gao, F. Yu, H. Zhou, et al., Direct synthesis and characterization of carbon nanotube films prepared by premixed ethanol flame, in: 3rd International, Conference on Manufacturing Science and Engineering ICMSE 20122012, Xiamen, 2016, pp. 569–573.

[37] A. Fraczek-Szczypta, E. Dlugon, A. Weselucha-Birczynska, M. Nocun, M. Blazewicz, Multi walled carbon nanotubes deposited on metal substrate using EPD technique. A spectroscopic study, J. Mol. Struct. 1040 (2013) 238–245.

[38] L. Vanyorek, R. Meszaros, S. Barany, Surface and electrosurface characterization of surface-oxidized multi-walled N-doped carbon nanotubes, Colloids Surf. A: Physicochem. Eng. Asp. 448 (1) (2014) 140–146.

[39] G. Yamamoto, J. Won Suk, J. An, R.D. Piner, T. Hashida, T. Takagi, R.S. Ruoff, The influence of nanoscale defects on the fracture of multi-walled carbon nanotubes under tensile loading, Diam. Relat. Mater. 19 (2010) 748–751.

[40] R. Yudianti, H. Onggo, Sudirman, Y. Saito, T. Iwata, J.I. Azuma, Analysis of functional group sited on multi-wall carbon nanotube surface, Open Mater. Sci. J. 5 (2011) 242–247.

[41] J. Zhang, H. Zou, Q. Qing, Y. Yang, Q. Li, Z. Liu, et al., Effect of chemical oxidation on the structure of single walled carbon nanotubes, J. Phys. Chem. B 107 (16) (2003) 3712–3718.

[42] R.J. Chen, Y. Zhang, D. Wang, H. Dai, Noncovalent sidewall functionalization of single-walled carbon nanotubes for protein immobilization, J. Am. Chem. Soc. 123 (16) (2001) 3838–3839.

[43] M.W. Marshall, S. Popa-Nita, J.G. Shapter, Measurement of functionalized carbon nanotube carboxylic acid groups using a simple chemical process, Carbon 44 (7) (2006) 1137–1141.